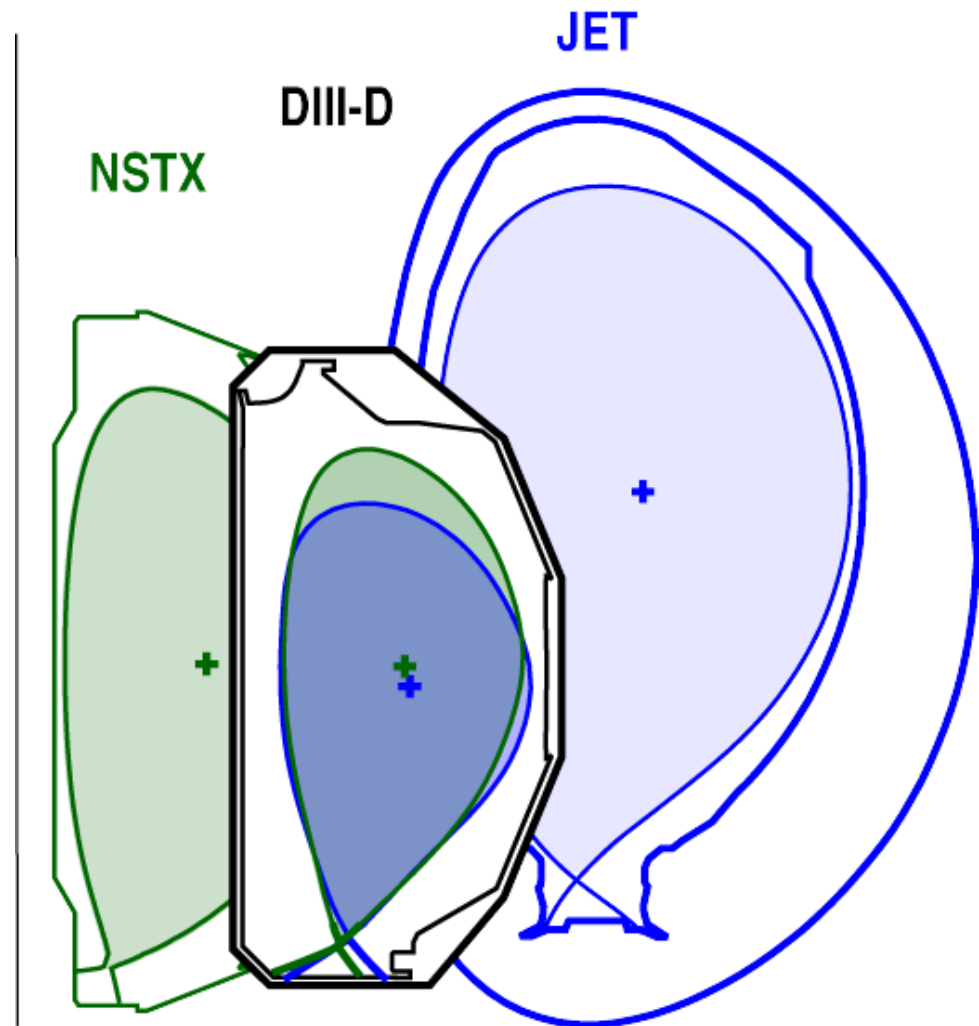


Cross-Machine Comparison of Resonant Field Amplification and Resistive Wall Mode Stabilization by Plasma Rotation

Presented by
H. Reimerdes

Presented at
Forty-Seventh Annual Meeting
American Physical Society
Division of Plasma Physics
Denver, Colorado

October 24–28, 2005



*Columbia
University*

Cross-Machine Comparison of Resonant Field Amplification and Resistive Wall Mode Stabilization by Plasma Rotation

In collaboration with

DIII-D team including

M.S. Chu, A.M. Garofalo, G.L. Jackson, R.J. La Haye, G.A. Navratil, M. Okabayashi, E.J. Strait, P. Gohil, R.J. Groebner, J.T. Scoville and W.M. Solomon

JET-EFDA contributors including

T.C. Hender, M.P. Gryaznevich, D.F. Howell, Y.Q. Liu, S.D. Pinches, M. Bigi, M. de Baar and P. de Vries

NSTX team including

S.A. Sabbagh, J.M. Bialek, J.E. Menard, A.C. Sontag, W. Zhu, D.A. Gates, D. Mueller and R. Raman

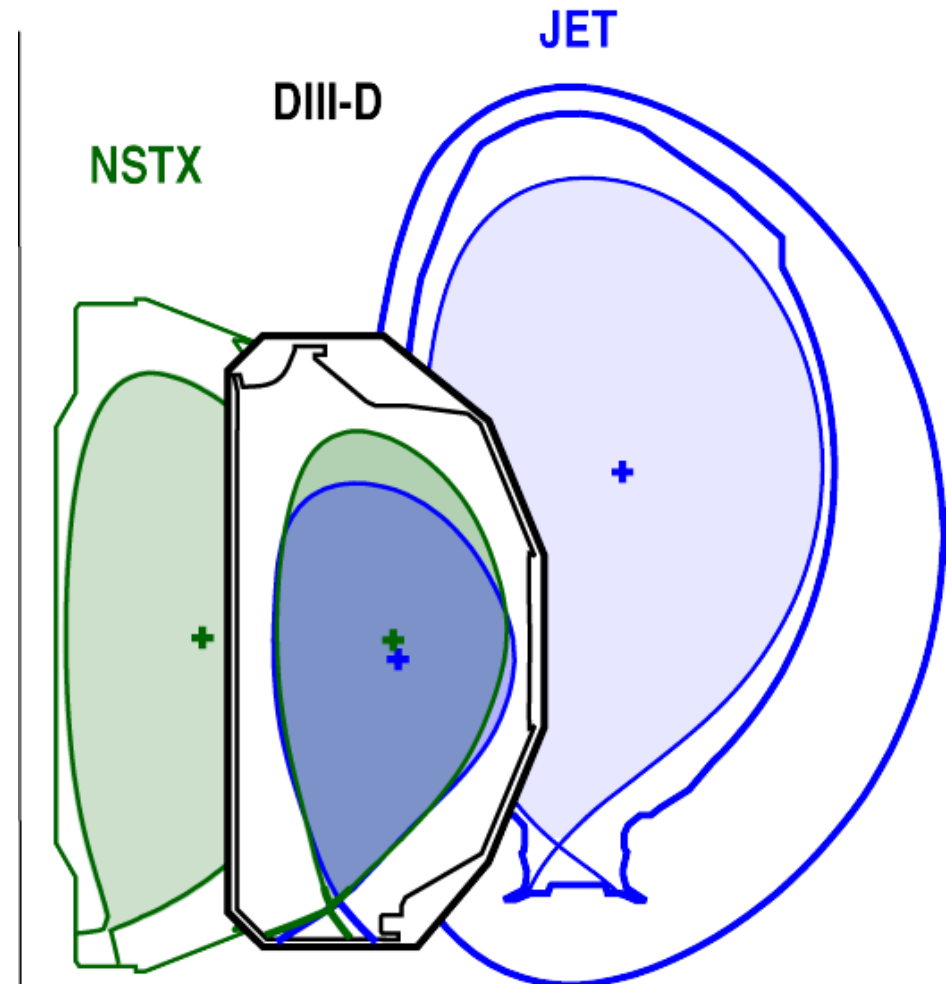


EUROPEAN FUSION DEVELOPMENT AGREEMENT
JET



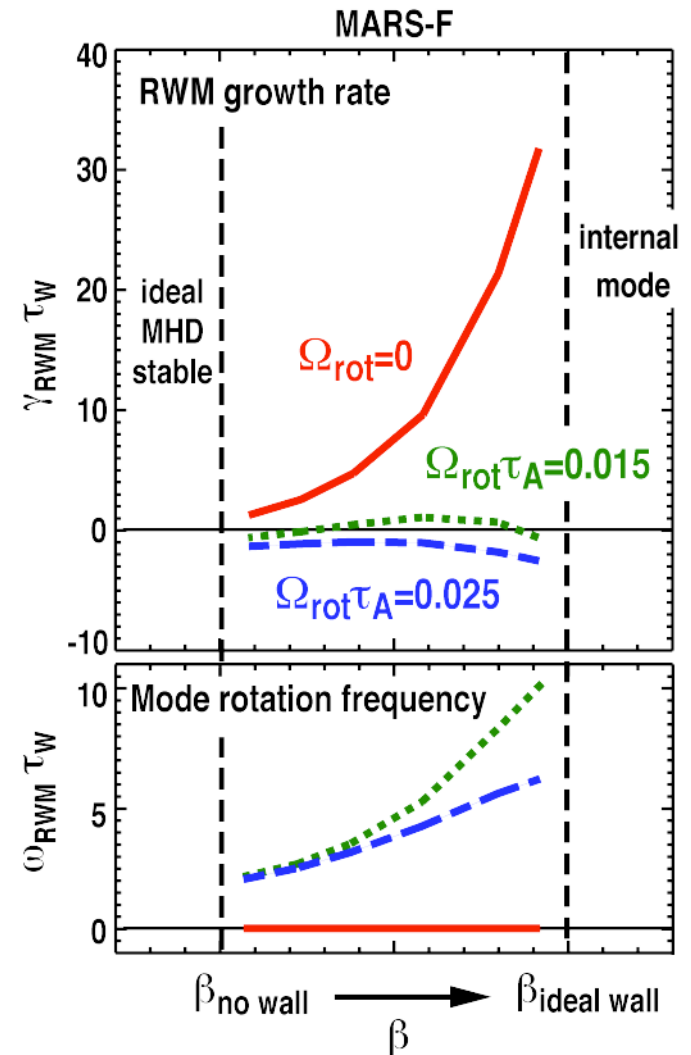
Cross-machine comparison establishes universality of resistive wall mode stabilization by plasma rotation

- Resistive wall mode (RWM) stabilization by plasma rotation has been studied up to high β_N
 - **NSTX**: $\beta_N \leq 7.3$
 - **DIII-D**: $\beta_N \leq 4.3$
 - **JET**: $\beta_N \leq 3.7$
- Recent DIII-D experiments demonstrate sustained $\beta_N \sim 4$ with active error field correction
 - A.M. Garofalo invited talk, UI2, Friday 9:30AM
- The devices vary in size and aspect ratio $A=R/a$



Plasma rotation can stabilize RWM up to the ideal wall stability limit

- **Resistive Wall Mode (RWM):**
 - External kink mode whose growth is slowed by magnetic field penetration through the conducting wall
 - Quasi-static perturbation in a fast toroidal plasma flow: $\gamma_{\text{RWM}}, \omega_{\text{RWM}} \sim \tau_{\text{W}}^{-1} \ll \Omega_{\text{rot}}$
- **Stabilizing effect of plasma rotation first observed in DIII-D** [E.J. Strait et al, PRL 74 (1995)]
 - Stabilization requires a dissipation mechanism [A. Bondeson, D.J. Ward, PRL 72 (1994)]
- **Resonant field amplification (RFA):**
 - Externally applied resonant fields can excite the weakly damped RWM [A.H. Boozer, PRL 86 (2001)]



Machine-size comparison between DIII-D and JET and aspect ratio comparison between DIII-D and NSTX

- **Machine size comparison: DIII-D and JET vary by a factor of 1.7**
 - Same resonant field amplification (RFA)
 - Same critical plasma rotation for RWM stabilization
 - Importance of $q=2$ surface for rotational stabilization
- **Aspect ratio comparison: DIII-D and NSTX vary by a factor of 2**
 - Higher critical rotation at low aspect ratio explained by trapped particles not contributing to RWM stabilization
 - Alternatively, the RWM stabilization is determined by the sound wave velocity rather than the Alfvén velocity
- **Target plasmas designed for a large difference between no wall and ideal wall β limits rather than maximum β_N**



Match parameters for the RWM drive and for the dissipation mechanism

- Obtain the same external kink mode by matching the ideal MHD properties of the plasma: shape, q-profile, pressure profile

- Express RWM drive by the normalized gain in β

$$C_\beta = \frac{\beta - \beta_{no\ wall}}{\beta_{ideal\ wall} - \beta_{no\ wall}} = \begin{cases} 0 & \text{at no wall limit} \\ 1 & \text{at ideal wall limit} \end{cases}$$

- Stabilization models:

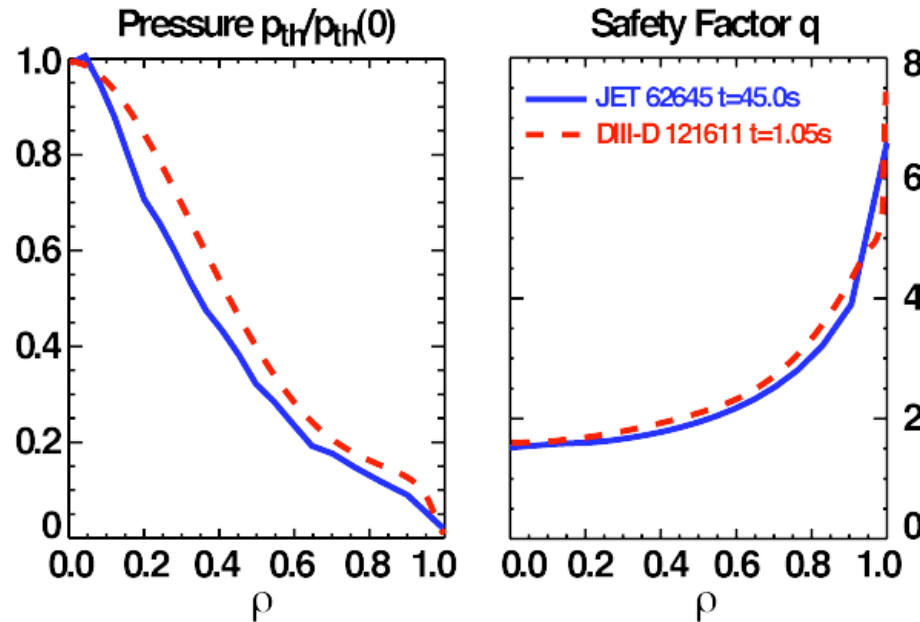
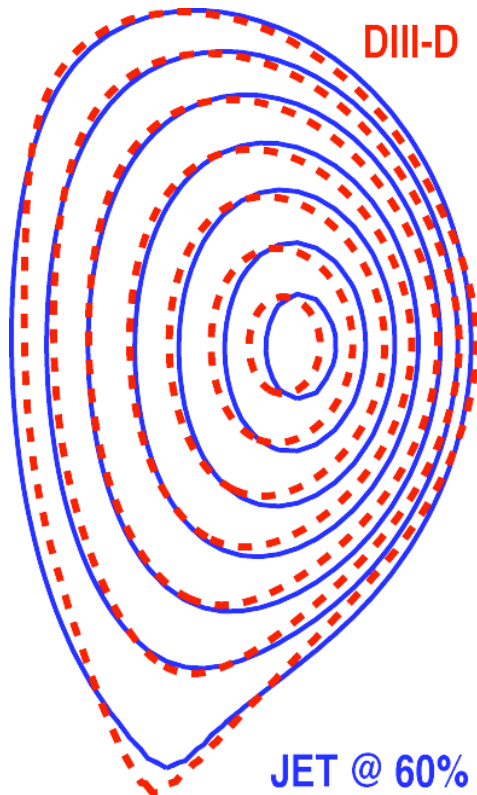
- **Sound wave damping:** Fluid approximation, where RWM couples to sound waves, which are then ion Landau damped, described via a parallel viscous force

- **Kinetic description** of inertia enhancement and ion Landau damping

→ **Normalize plasma rotation frequency with inverse of Alfvén time**

$$\tau_A = R_0 \frac{\sqrt{\mu_0 n_e m_i}}{B_0}$$

Matching shape and profiles leads to same ideal MHD no-wall stability limit in DIII-D and JET plasmas



- **ELMy H-mode target plasma**
 - $q_0 \approx 1.5$
 - $q_{95} = 3.3 - 5.0$
 - $\ell_i \approx 0.7$ (DIII-D) / 0.95 (JET)
 - $\beta_{N, no\ wall} \sim 2.8 \ell_i$ in DIII-D and JET
- **Ideal MHD no-wall stability limit:**

Wall-stabilized regime in DIII-D and JET varies due to different ℓ_i and wall geometry

- **No wall stability limit**

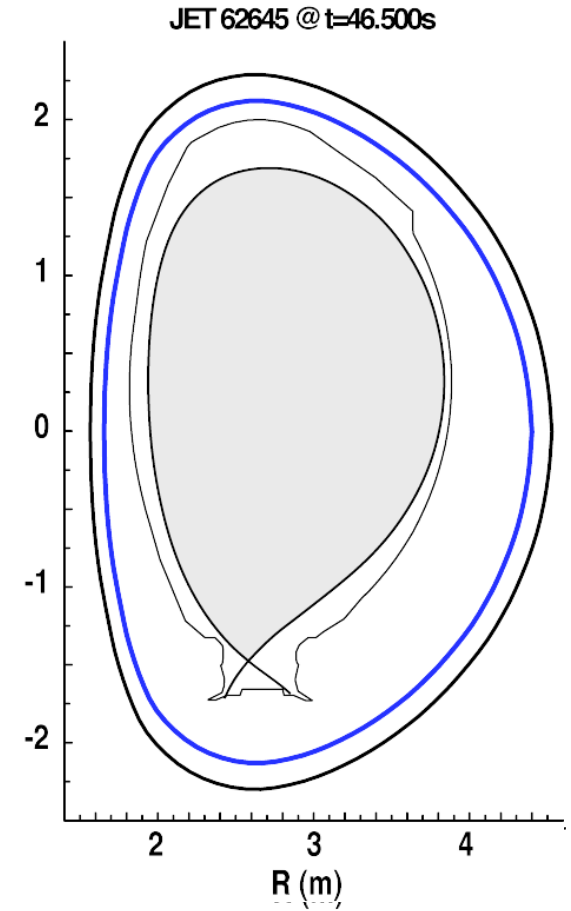
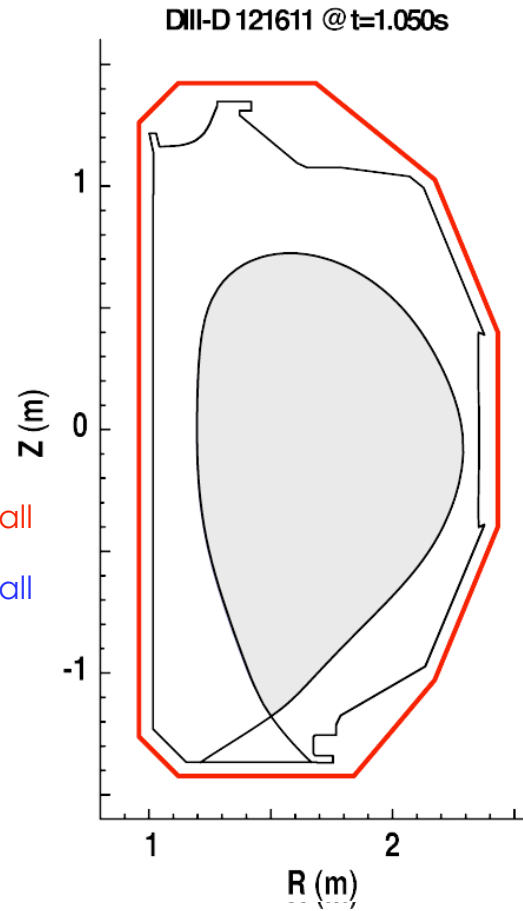
DIII-D: $\beta_{N,\text{no wall}} \approx 2.0$

JET: $\beta_{N,\text{no wall}} \approx 2.7$

- **Ideal wall stability limit**

DIII-D: $\beta_{N,\text{ideal wall}} \approx 1.5 \beta_{N,\text{no wall}}$

JET: $\beta_{N,\text{ideal wall}} \approx 1.3 \beta_{N,\text{no wall}}$



Wall-stabilized regime in DIII-D and JET varies due to different ℓ_i and wall geometry

- **No wall stability limit**

DIII-D: $\beta_{N,no\ wall} \approx 2.0$

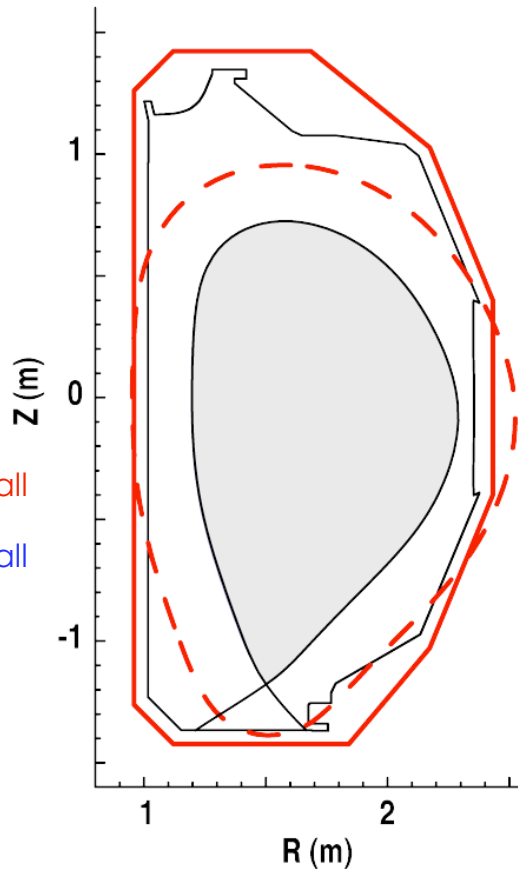
JET: $\beta_{N,no\ wall} \approx 2.7$

- **Ideal wall stability limit**

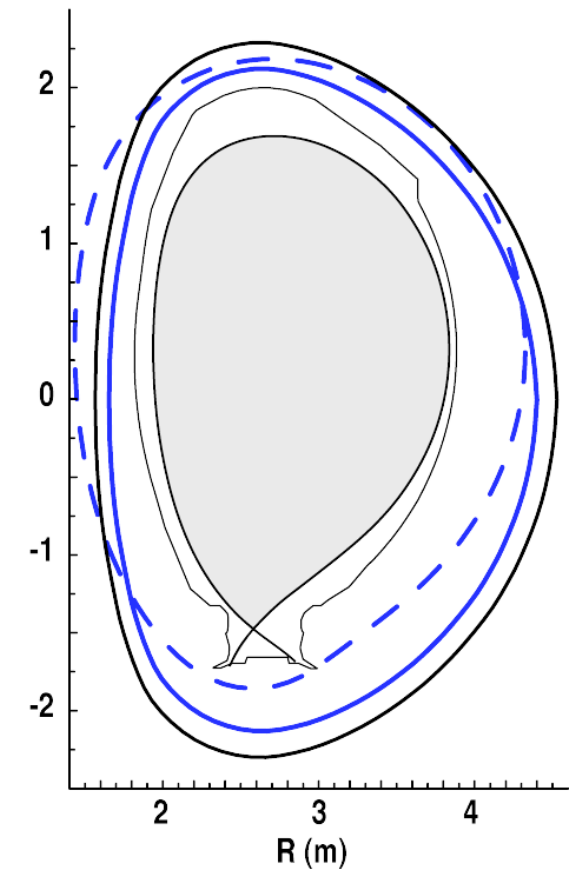
DIII-D: $\beta_{N,ideal\ wall} \approx 1.5 \beta_{N,no\ wall}$

JET: $\beta_{N,ideal\ wall} \approx 1.3 \beta_{N,no\ wall}$

DIII-D 121611 @ t=1.050s



JET 62645 @ t=46.500s



- **Effective conformal wall:**

$d_c \approx 0.45a$ (DIII-D)

$d_c \approx 0.55a$ (JET)

DIII-D and NSTX develop common target with a substantial wall-stabilized regime

- Profiles are not well matched due to aspect ratio effects

- No wall stability limit

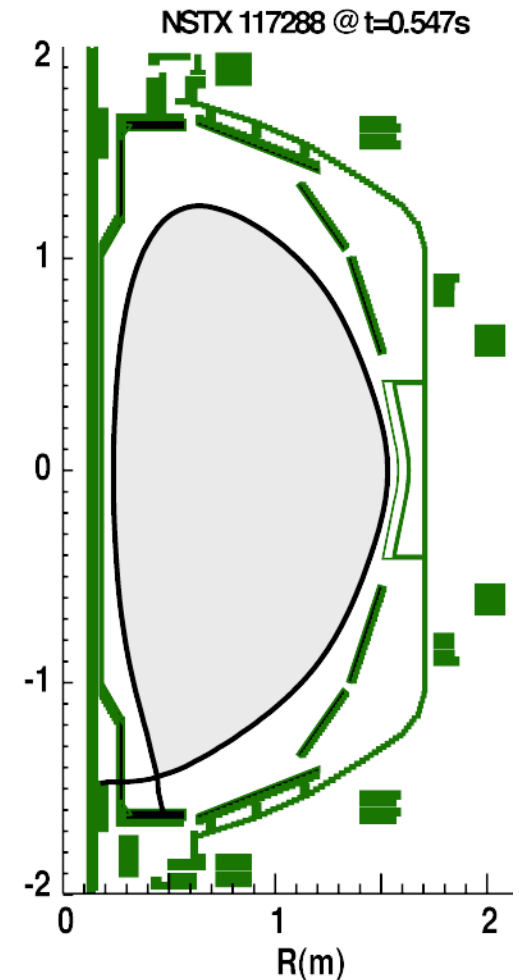
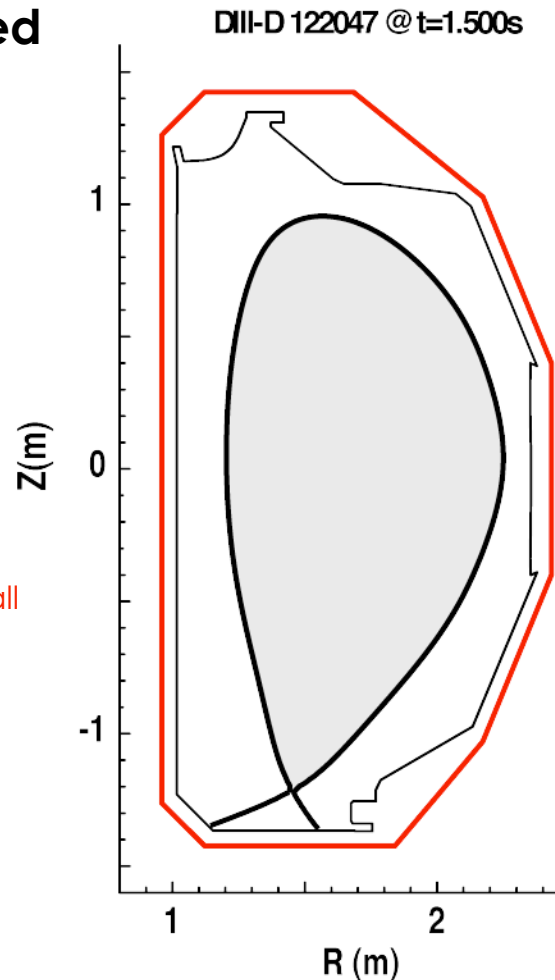
DIII-D: $\beta_{N, \text{no wall}} \approx 2.0$

NSTX: $\beta_{N, \text{no wall}} \approx 4.0-4.8$

- Ideal wall stability limit

DIII-D: $\beta_{N, \text{ideal wall}} \approx 1.5 \beta_{N, \text{no wall}}$

NSTX: $\beta_{N, \text{ideal wall}} \approx 1.3 - 1.5 \beta_{N, \text{no wall}}$



DIII-D and NSTX develop common target with a substantial wall-stabilized regime

- Profiles are not well matched due to aspect ratio effects

- No wall stability limit

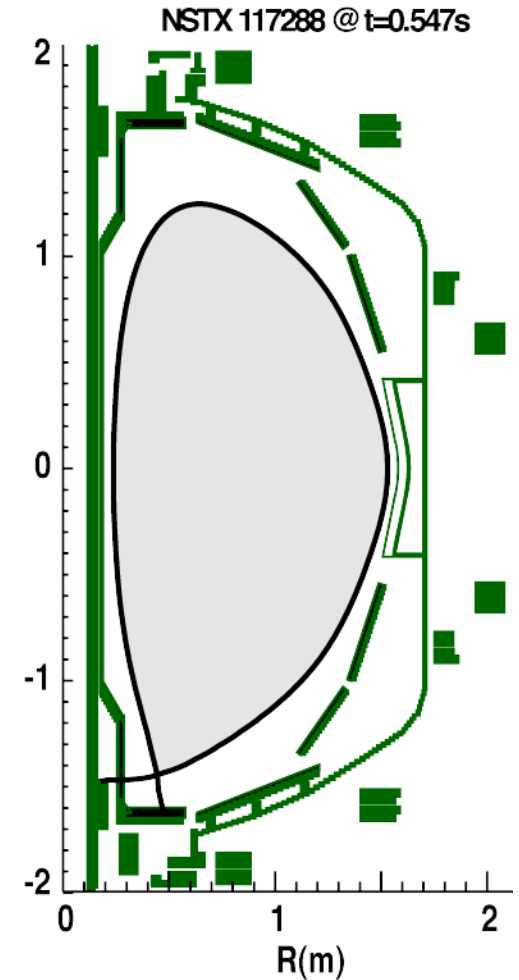
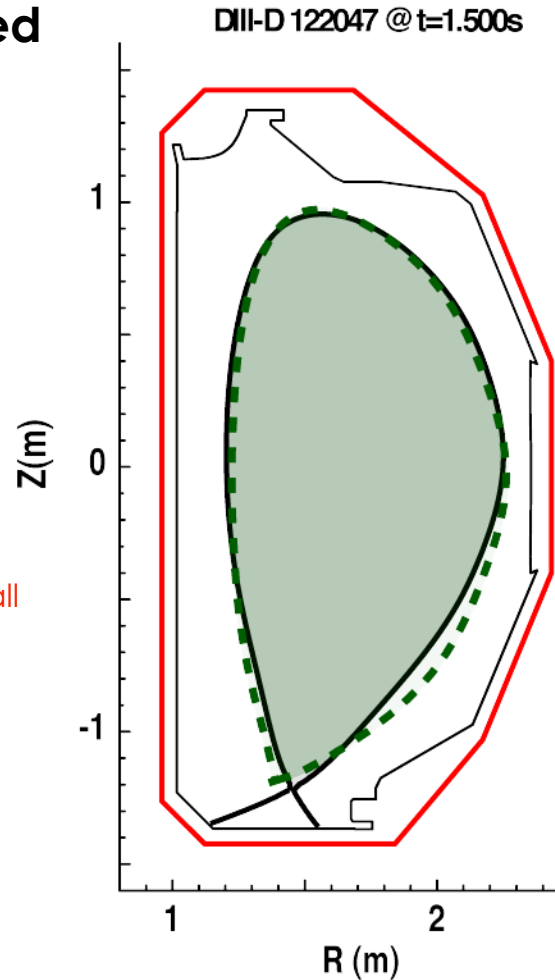
DIII-D: $\beta_{N, \text{no wall}} \approx 2.0$

NSTX: $\beta_{N, \text{no wall}} \approx 4.0-4.8$

- Ideal wall stability limit

DIII-D: $\beta_{N, \text{ideal wall}} \approx 1.5 \beta_{N, \text{no wall}}$

NSTX: $\beta_{N, \text{ideal wall}} \approx 1.3 - 1.5 \beta_{N, \text{no wall}}$



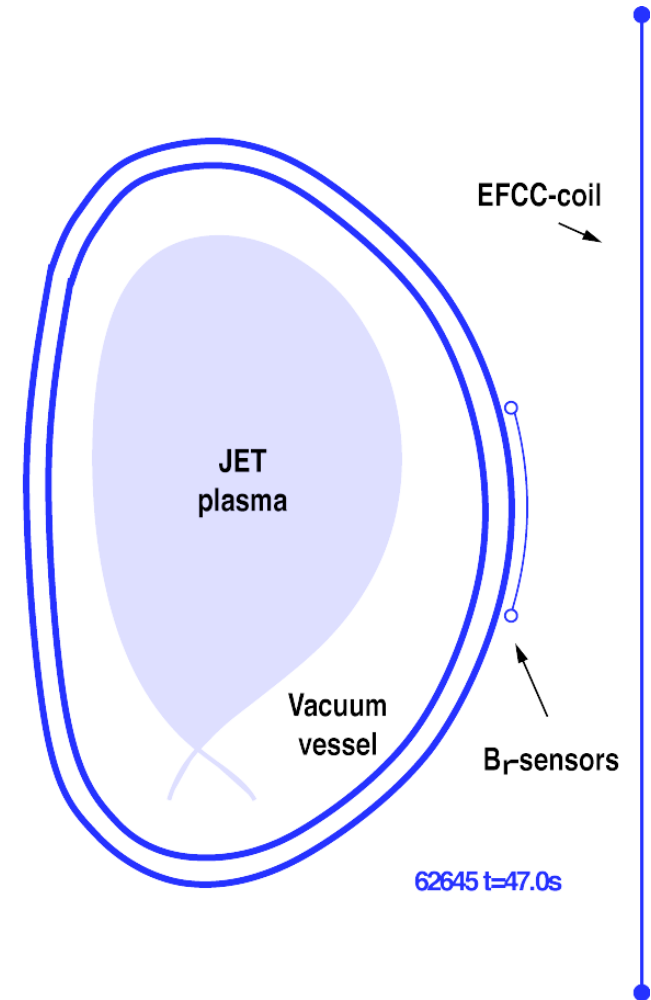
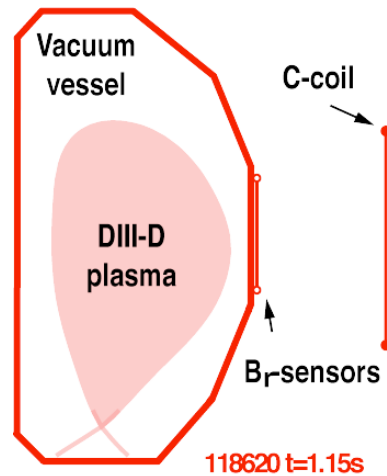
Machine-size comparison between DIII-D and JET and aspect ratio comparison between DIII-D and NSTX

- **Machine size comparison: DIII-D and JET vary by a factor of 1.7**
 - Same resonant field amplification (RFA)
 - Same critical plasma rotation for RWM stabilization
 - Importance of $q=2$ surface for rotational stabilization
- **Aspect ratio comparison: DIII-D and NSTX vary by a factor of 2**
 - Higher critical rotation at low aspect ratio explained by trapped particles not contributing to RWM stabilization
 - Alternatively, the RWM stabilization is determined by the sound wave velocity rather than the Alfvén velocity



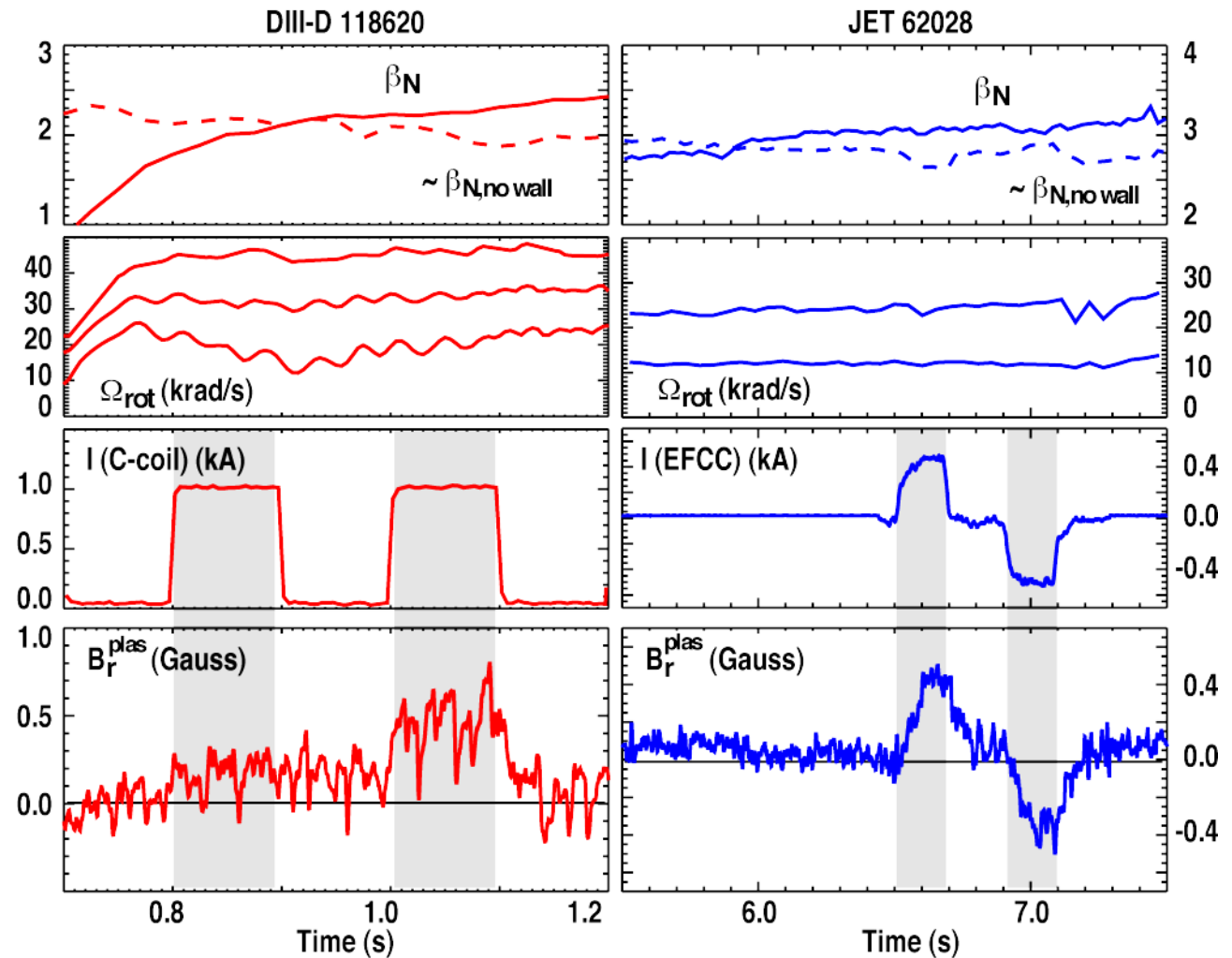
DIII-D and JET plasmas probed using non-axisymmetric external control coils with similar geometry

- Apply resonant field pulses B^{ext} with one pair of external control coils (predominantly $n=1$)
- Detect plasma response B^{plas} with toroidal arrays of B_r sensors



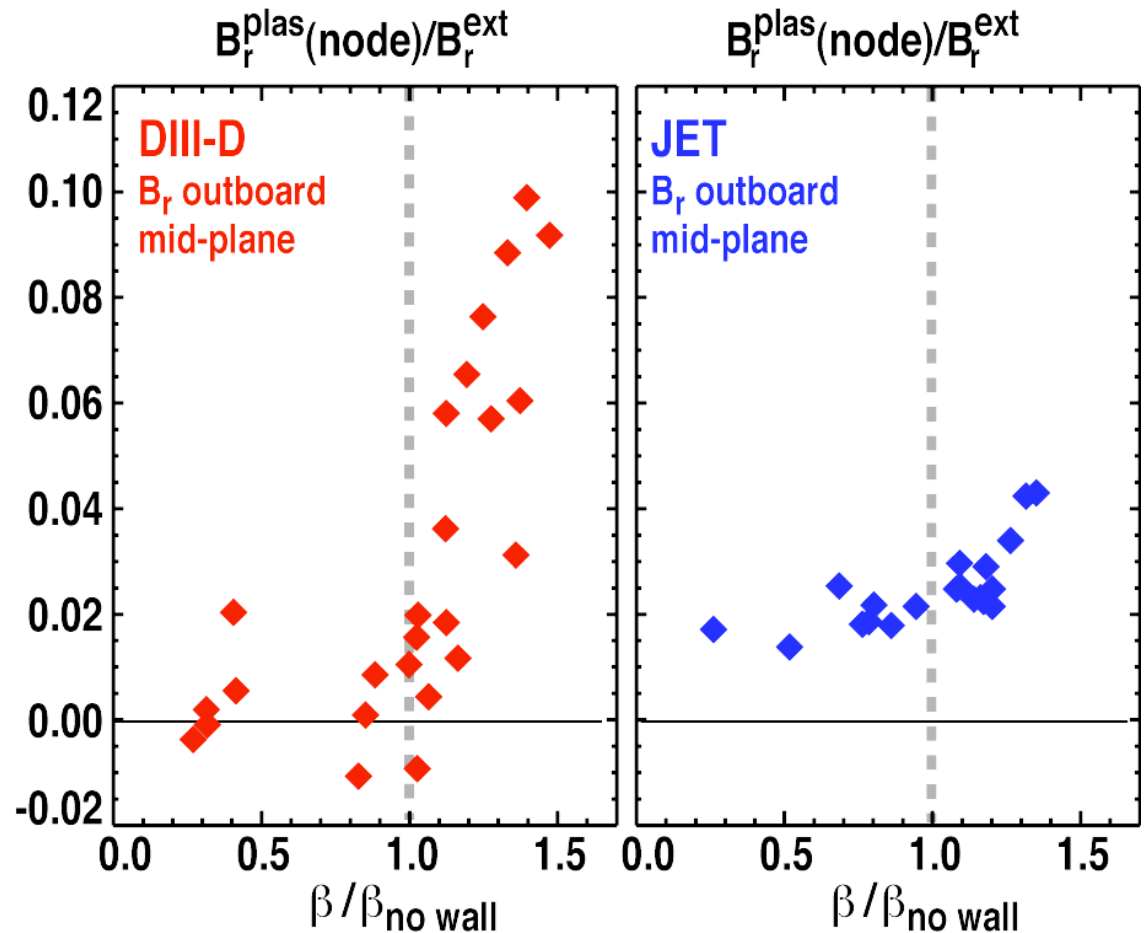
High- β plasmas respond to externally applied $n=1$ perturbations

- Beta exceeds no-wall limit
- Plasma rotation provides RWM stabilization
- Probe plasma with externally applied $n=1$ field
- RFA leads to plasma response detected at the (toroidal) node of the applied field



RFA in DIII-D and JET increase significantly once β exceeds no wall stability limit

- Increase of RFA for $\beta > \beta_{\text{no-wall}}$ consistent with previous observations in DIII-D and NSTX [A.C. Sontag et al, Phys. Plasmas (2005)]
 - Low β response in JET differs from DIII-D
- Measured amplification in DIII-D twice as large as in JET

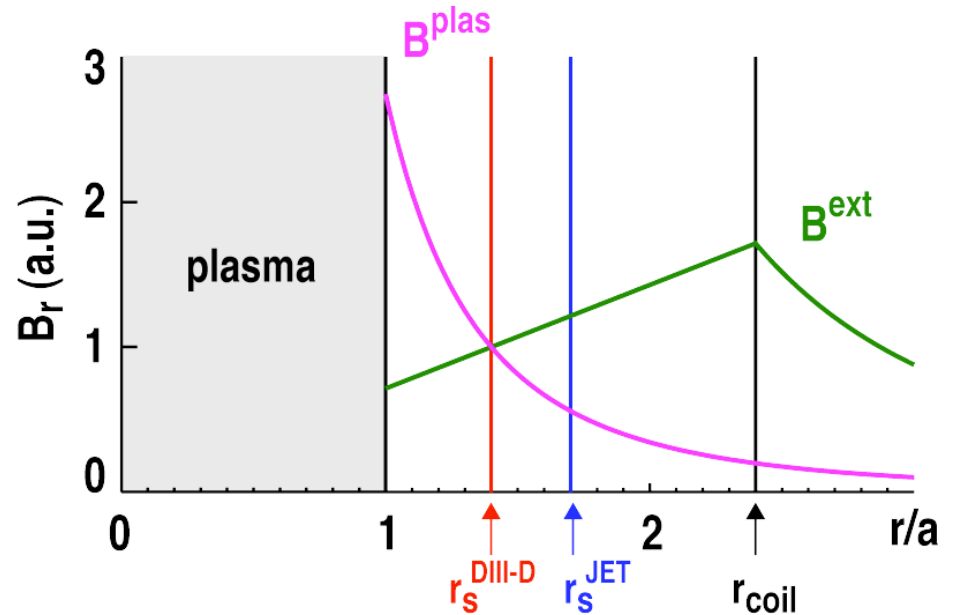


Comparison of RFA measurements has to account for geometry of magnetic fields and sensor locations

- Similar geometry of applied fields in DIII-D and JET
- Similar geometry of plasma perturbation in DIII-D and JET
- Radial decay of external field and plasma response cause radial dependence of B^{plas}/B^{ext}
 - Cylindrical approximation

$$\frac{B_a^{plas}/B_a^{ext}}{B_s^{plas}/B_s^{ext}} = \left(r_s/a\right)^{2m}$$

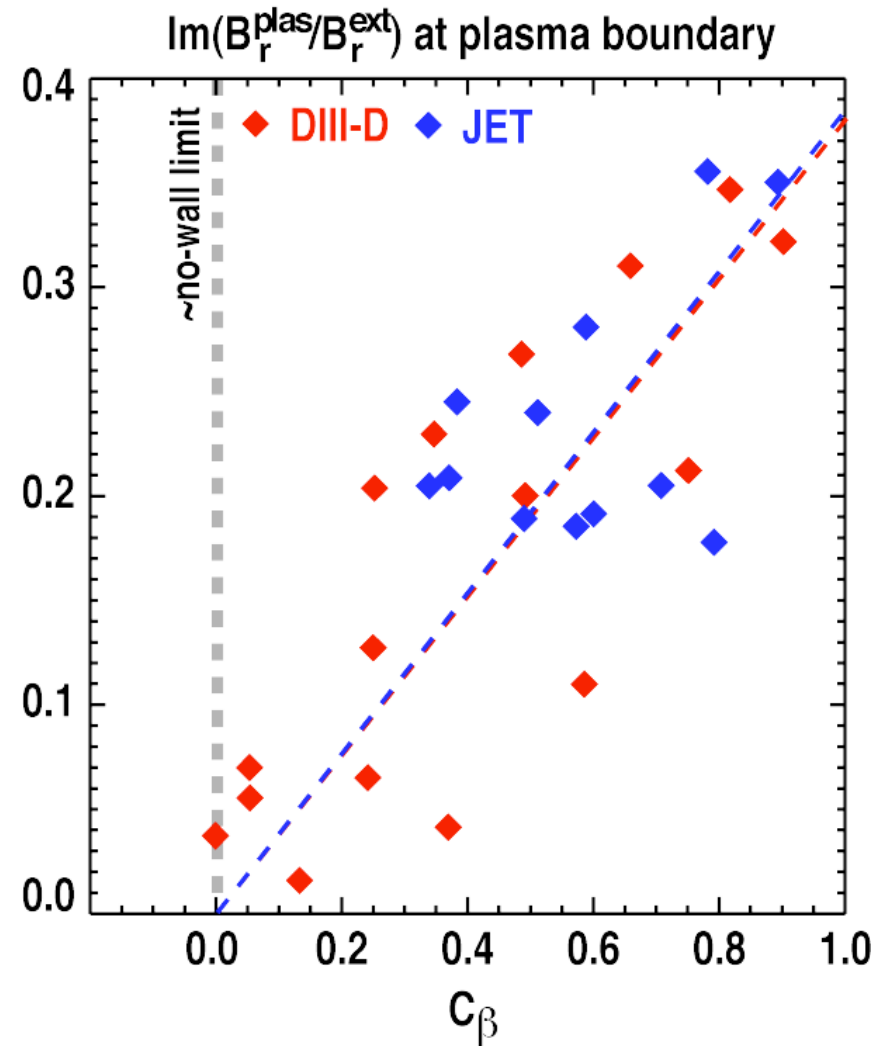
- Assume effective poloidal mode number $m=2$ at outboard midplane



	DIII-D	JET
a (m)	0.54	0.95
r_s (m)	0.74	1.61
$(r_s/a)^4$	3.5	8.25

RFA magnitudes at the plasma boundary in DIII-D and JET are in quantitative agreement

- Map RFA to the same location, e.g. plasma boundary
- RWM drive described by normalized gain over no wall limit C_β

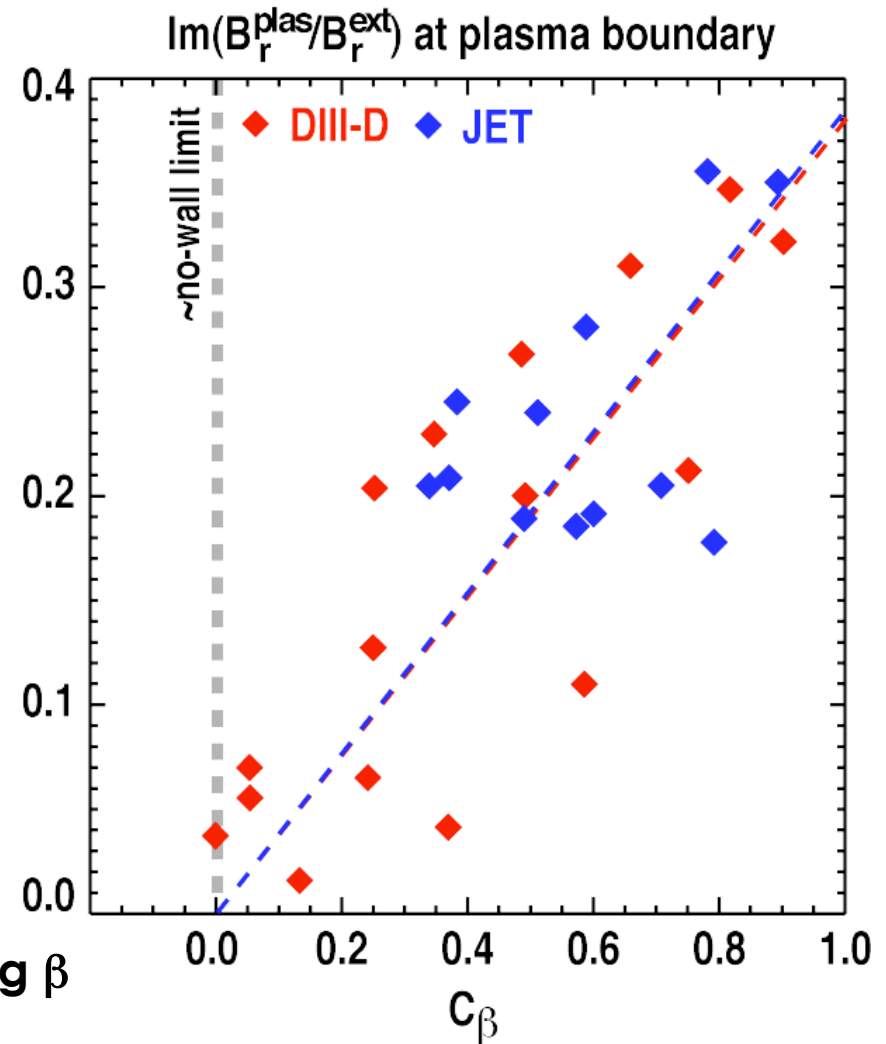


RFA magnitudes at the plasma boundary in DIII-D and JET are in quantitative agreement

- Map RFA to the same location, e.g. plasma boundary
- RWM drive described by normalized gain over no wall limit C_β
- Link quantitative agreement of RFA to RWM damping rate $-\gamma_{RWM}$

$$\frac{B_s^{plas}(\text{node})}{|B_s^{ext}|} \propto \frac{\omega_{RWM}\tau_W}{(\gamma_{RWM}\tau_W)^2 + (\omega_{RWM}\tau_W)^2}$$

- RWM in DIII-D and JET equally damped by plasma rotation
- Weaker RWM damping with increasing β



Machine-size comparison between DIII-D and JET and aspect ratio comparison between DIII-D and NSTX

- **Machine size comparison: DIII-D and JET vary by a factor of 1.7**
 - Same resonant field amplification (RFA)
 - Same critical plasma rotation for RWM stabilization
 - Importance of $q=2$ surface for rotational stabilization
- **Aspect ratio comparison: DIII-D and NSTX vary by a factor of 2**
 - Higher critical rotation at low aspect ratio explained by trapped particles not contributing to RWM stabilization
 - Alternatively, the RWM stabilization is determined by the sound wave velocity rather than the Alfvén velocity



Braking of plasma rotation needed for RWM onset

- NBI torque in NSTX, DIII-D and JET is usually provides sufficient rotation for RWM stabilization
- Increase drag by applying non-axisymmetric fields

- Neoclassical toroidal viscosity (NTV)

[Shaing, Phys. Plasmas 10, 1443 (2003)] :

$$T_{NTV} \propto (\delta B/B)^2$$

- Non-linear RWM onset

- Magnetic braking:

$$\frac{d}{dt} \Omega_{rot} \propto \delta B^2$$

- RWM dispersion relation:

$$\gamma_{RWM} \tau_W = f(\Omega_{rot})$$

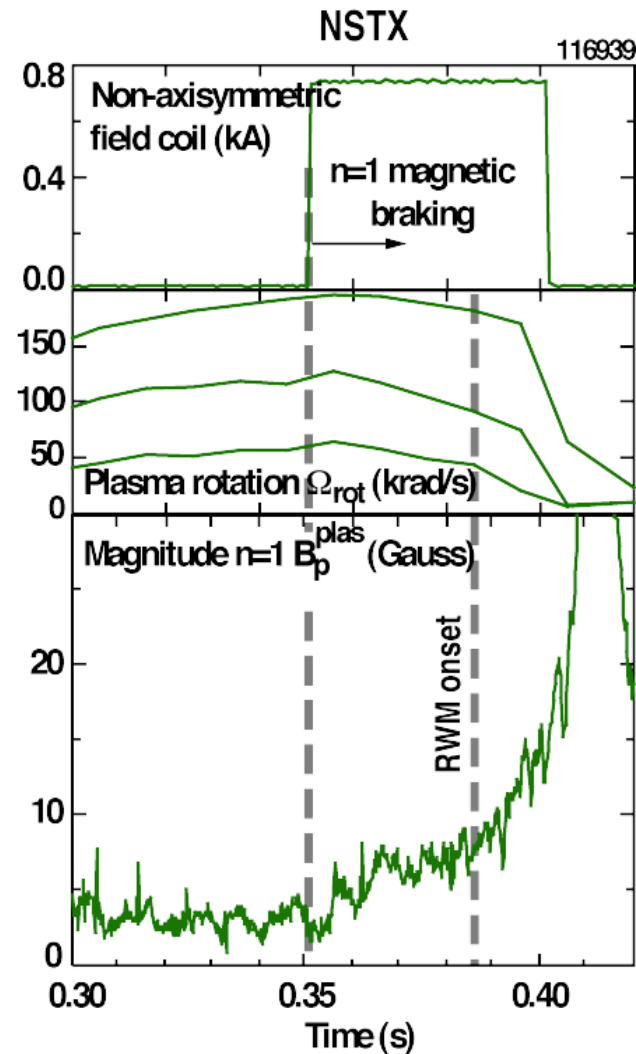
- Evolution of perturbed field (RFA and RWM):

$$\tau_W \left(\frac{d}{dt} \delta B - \gamma_{RWM} \delta B \right) = \delta B^{ext}$$

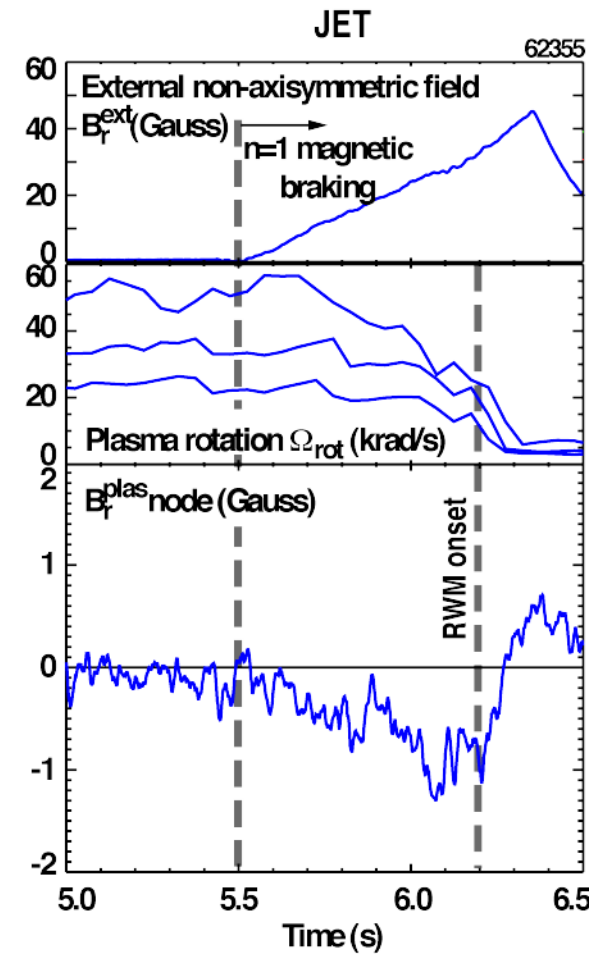
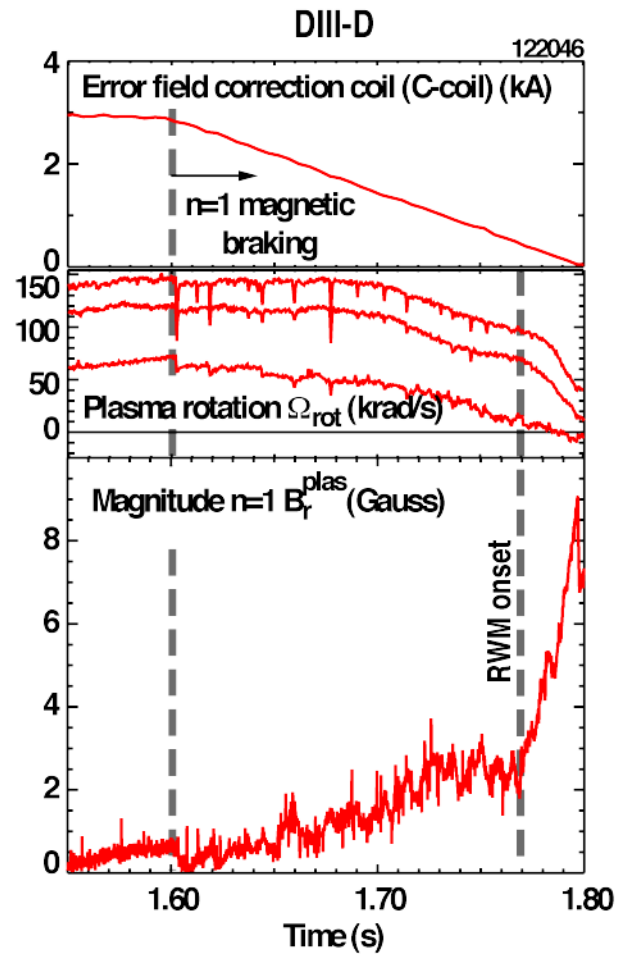
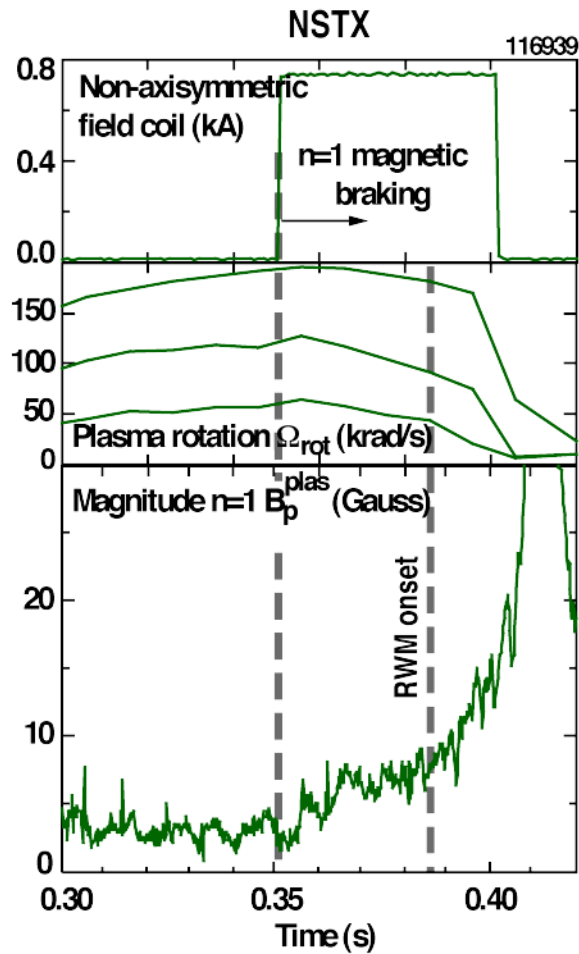


Magnetic braking leads to non-linear RWM onset

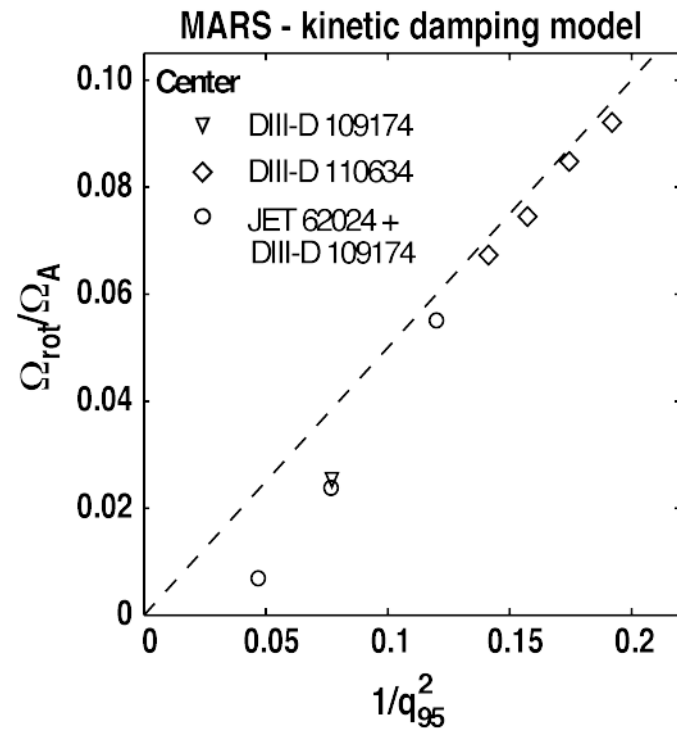
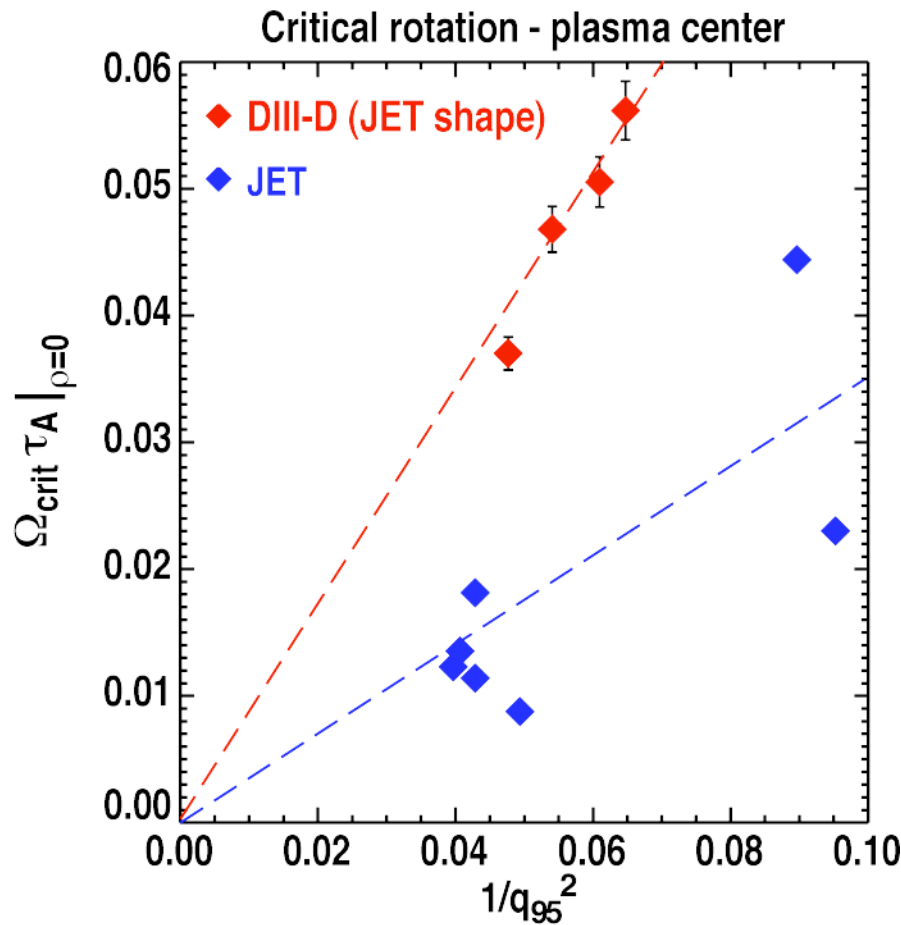
- Apply $n=1$ field
 - Plasma rotation decreases
 - Onset of fast growth is preceded by increasing RFA
- ↓
- Critical rotation Ω_{crit} measured at onset of fast growth



Time of marginal stability determined from start of fast mode growth



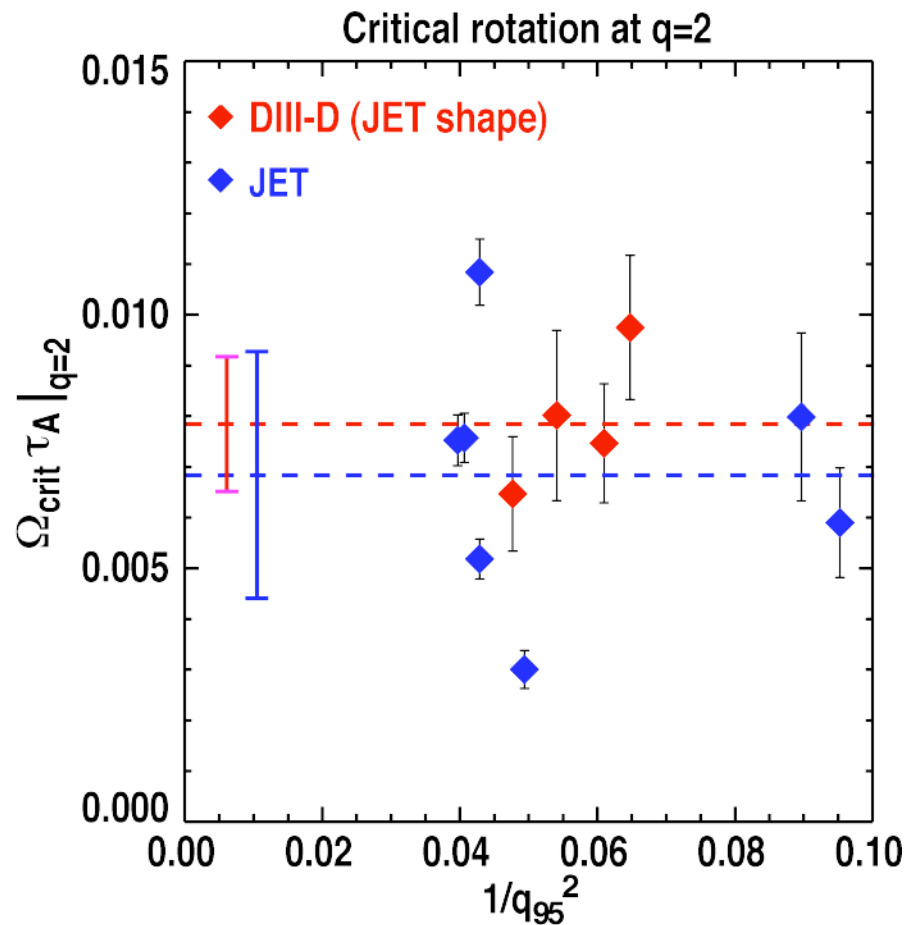
Critical rotation in the center of DIII-D and JET plasmas decreases with increasing q_{95}



- q_{95} -dependence consistent with MARS-F predictions

→ Y.Q. Liu, next talk

Evaluating Ω_{crit} at $q=2$ removes q_{95} -dependence and leads to quantitative agreement between DIII-D and JET

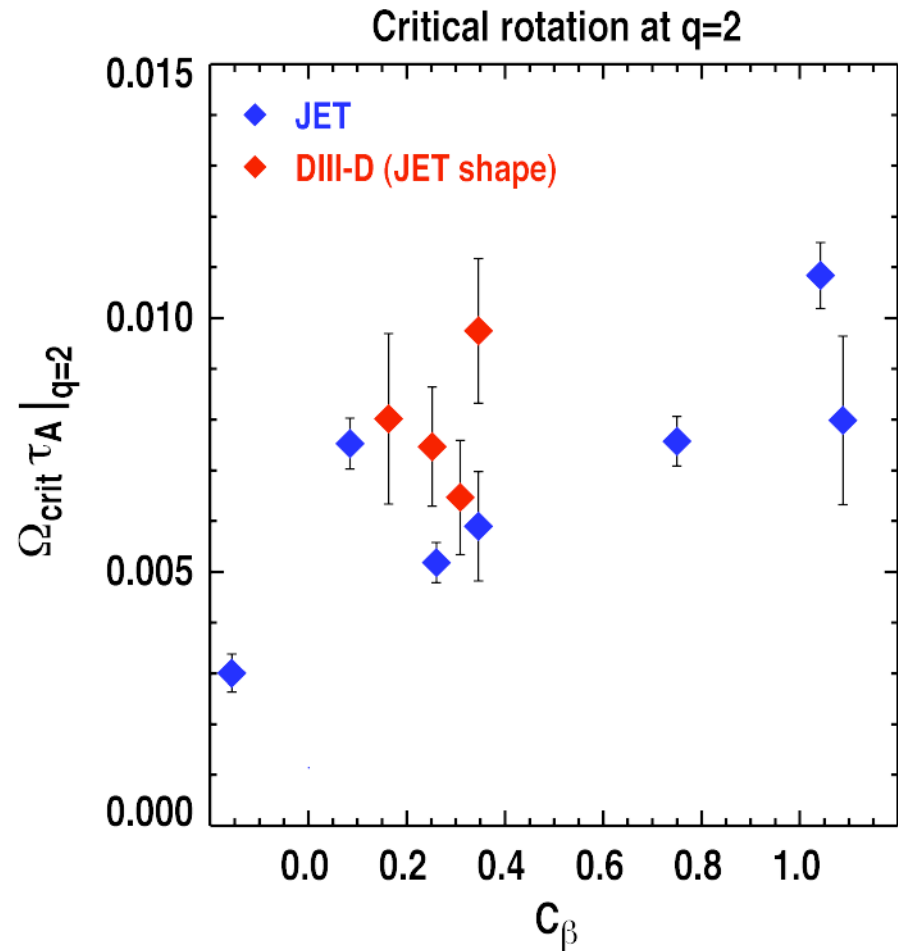


- q_{95} -dependence caused by q -surfaces moving inwards towards higher rotation
 - Stabilization mechanism depends on local q , e.g. kinetic damping [A. Bondeson and M.S. Chu, Phys. Plasmas (1996)],

$$\Omega_{crit} \propto 1/q^2$$
- Quantitative agreement in DIII-D and JET indicates prominent role of $q=2$ surface
 - Consistent with predictions for sound wave damping [D. Gregoratto, et al, Plasma Phys. Control. Fusion (2001)]
- Variations of JET data partially caused by β -dependence

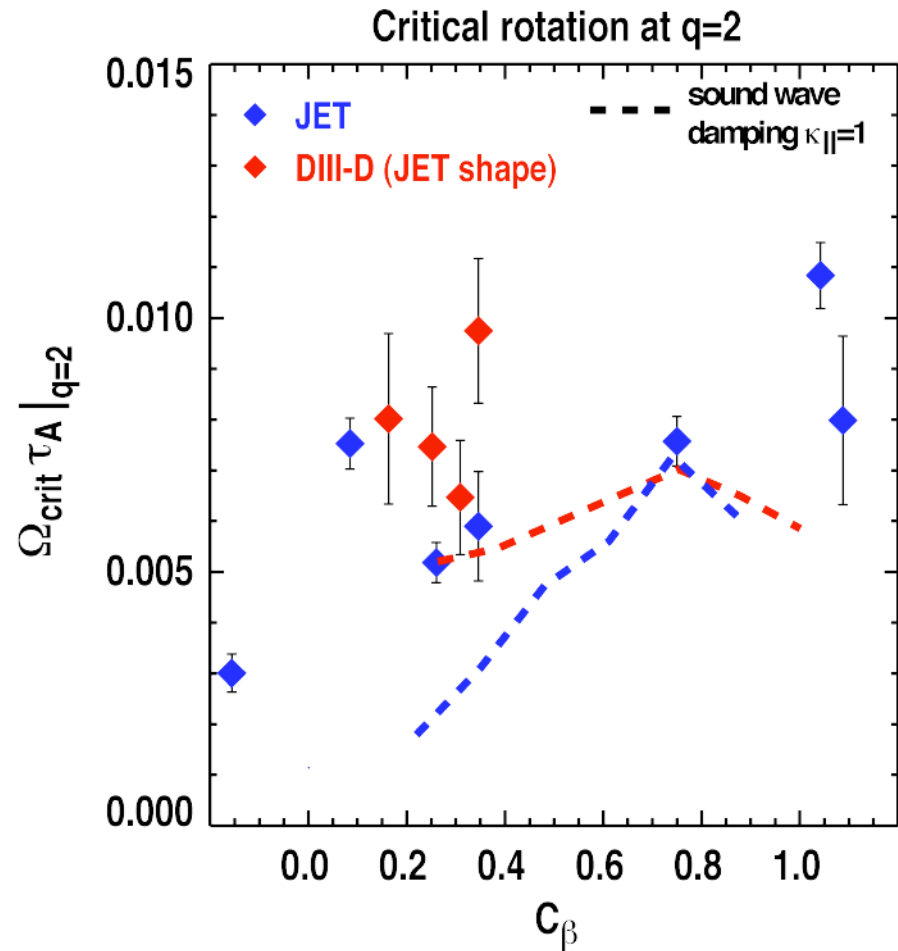
Ω_{crit} has weak β -dependence

- Beta-dependence of Ω_{crit} can account for some of the scatter of the measurement
- Consistent with increase of RFA with β



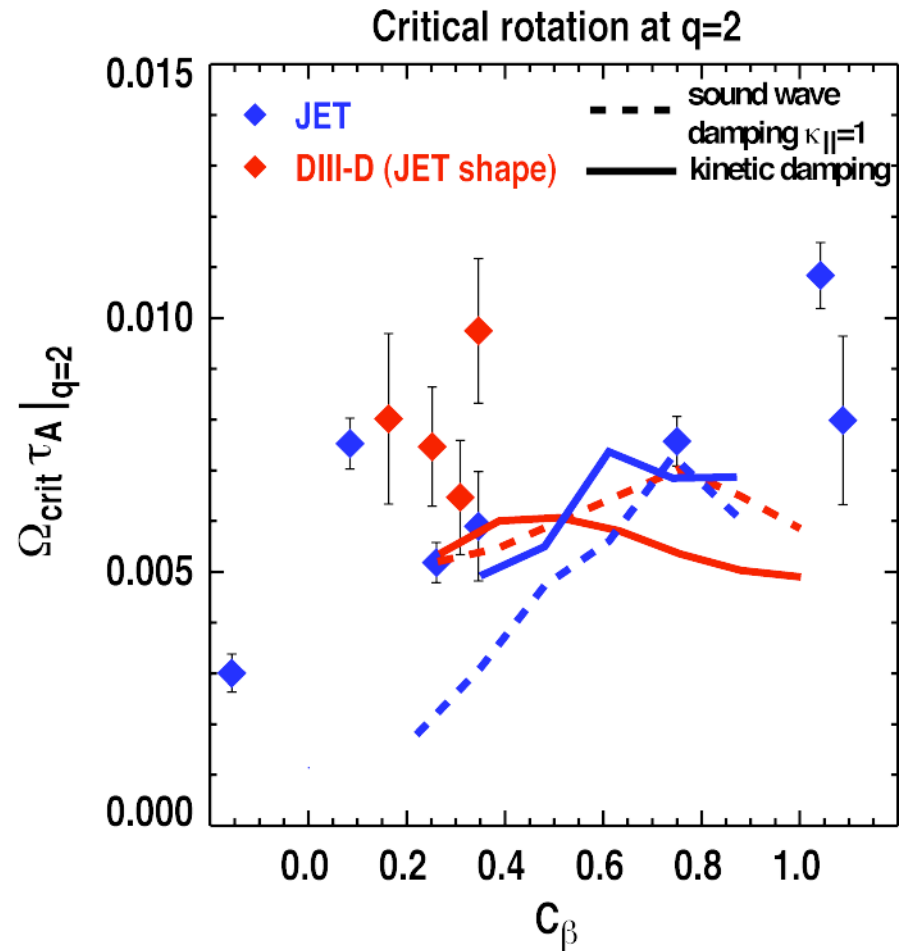
Ω_{crit} has weak β -dependence

- Beta-dependence of Ω_{crit} can account for some of the scatter of the measurement
- Consistent with increase of RFA with β
- Value of Ω_{crit} consistent with predictions (using MARS-F) for
 - Sound wave damping



Ω_{crit} has weak β -dependence

- Beta-dependence of Ω_{crit} can account for some of the scatter of the measurement
- Consistent with increase of RFA with β
- Value of Ω_{crit} consistent with predictions (using MARS-F) for
 - Sound wave damping
 - Kinetic damping



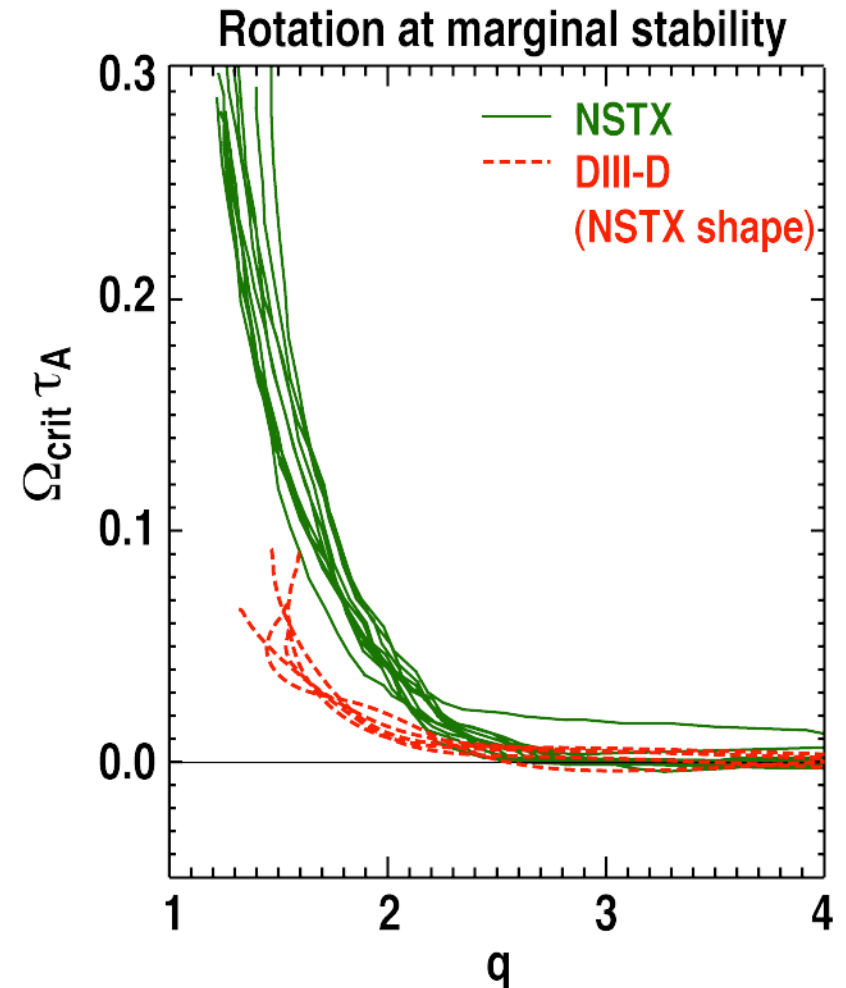
Machine-size comparison between DIII-D and JET and aspect ratio comparison between DIII-D and NSTX

- **Machine size comparison: DIII-D and JET vary by a factor of 1.7**
 - Same resonant field amplification (RFA)
 - Same critical plasma rotation for RWM stabilization
 - Importance of $q=2$ surface for rotational stabilization
- **Aspect ratio comparison: DIII-D and NSTX vary by a factor of 2**
 - Higher critical rotation at low aspect ratio explained by trapped particles not contributing to RWM stabilization
 - Alternatively, the RWM stabilization is determined by the sound wave velocity rather than the Alfvén velocity



Critical rotation in NSTX exceeds critical rotation in DIII-D

- q_{95} -dependence in NSTX similar to DIII-D and JET
- ↓
- Evaluate Ω_{crit} at the same value of q
- NSTX critical rotation $\Omega_{\text{crit}}\tau_A$ at same q always equal or higher
 - Rotation for $q \geq 3$ close to zero
- ↓
- Single resonant surface can be sufficient for RWM stabilization

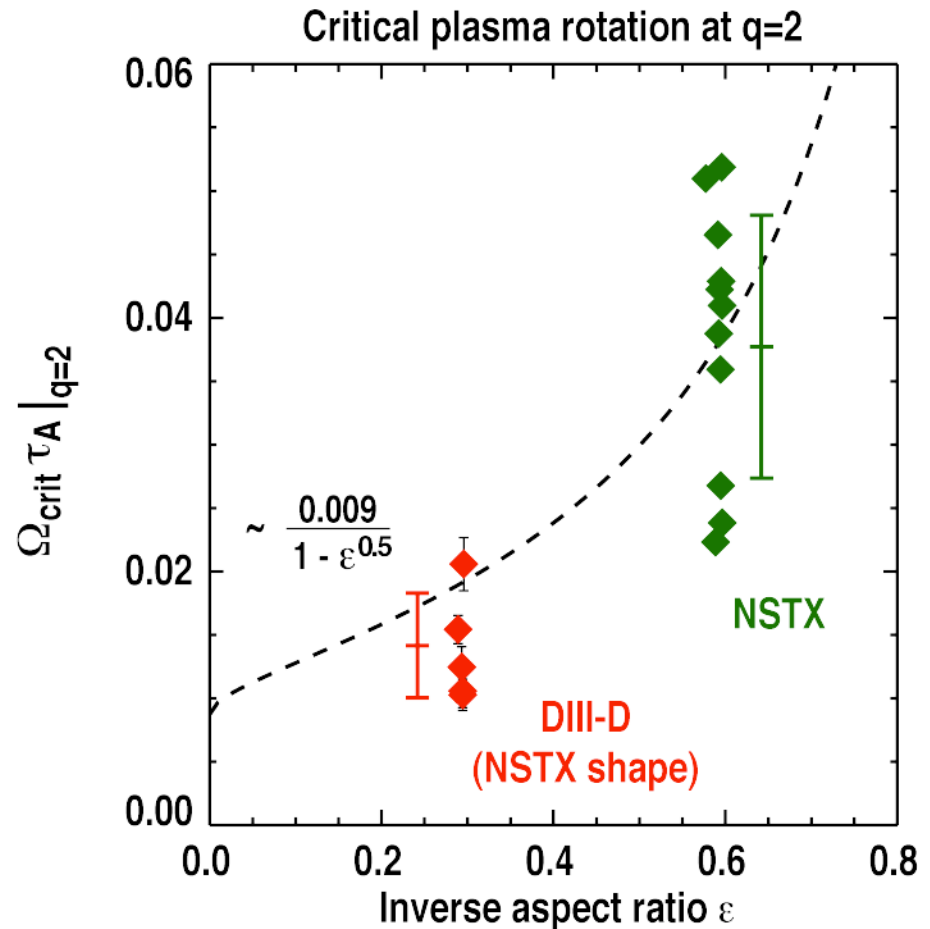


Aspect ratio dependence suggests that trapped particles do not contribute to RWM stabilization

- **Ion Landau damping significantly reduced for trapped particles**
 - Assume that only passing particles contribute to RWM stabilization

$$\Omega_{crit} \tau_A \propto \frac{1}{1 - \sqrt{\epsilon}}$$

- **Observed doubling of $\Omega_{crit} \tau_A$ consistent with stabilization by passing particles only**
 - Effect included in the kinetic but not in the sound wave damping model



Alternatively - RWM damping could be determined by sound wave velocity

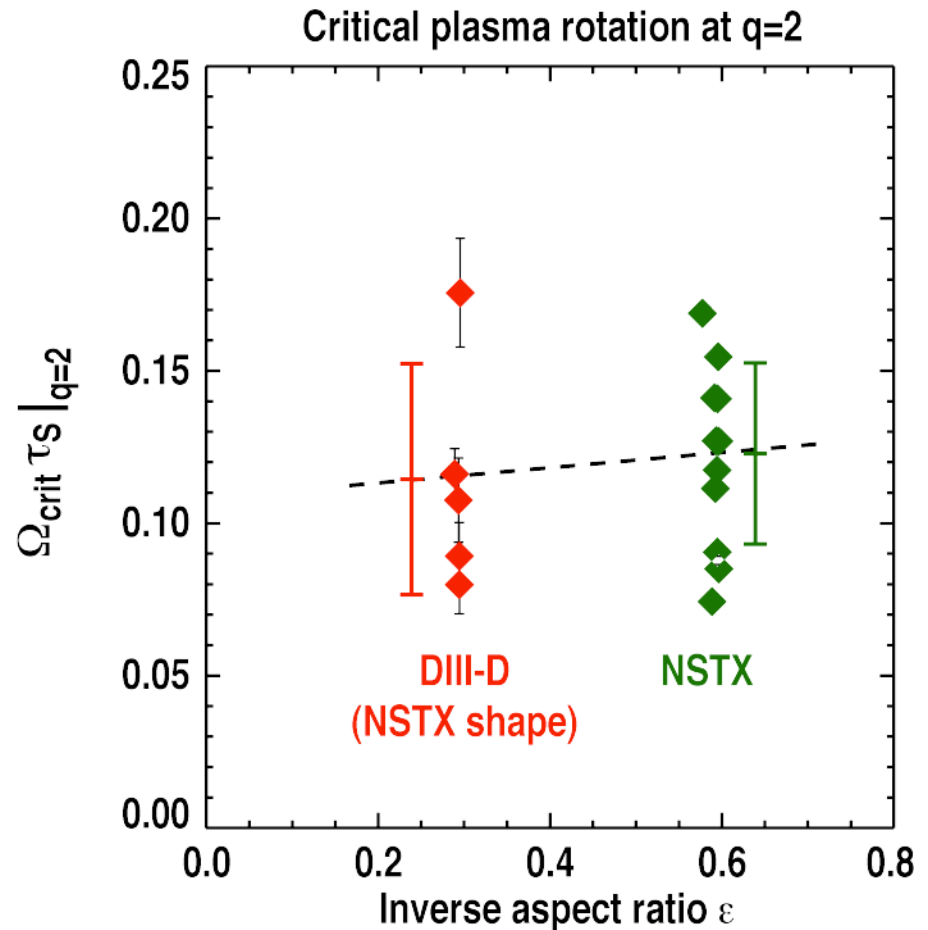
- Coupling to sound waves depends on sound time

$$\tau_S = R_0 \sqrt{\frac{m_i}{k_B T_e + k_B T_i}}$$

- Alfvén time and sound time linked via β

$$\frac{\tau_A}{\tau_S} \propto \beta^{1/2} \propto (\varepsilon \beta_N / q_{95})^{1/2}$$

- Link is broken by aspect ratio
- Normalization on sound time removes aspect ratio dependence



Comparison of NSTX, DIII-D and JET establishes universality of RWM stabilization by plasma rotation

- **q_{95} -dependence of $\Omega_{\text{crit}}\tau_A$ explained by re-location of q -surfaces**
 - RWM stabilization depends on the local q
- **Quantitative agreement of $\Omega_{\text{crit}}\tau_A$ evaluated at $q=2$ in DIII-D and JET**
 - Physics determined by ideal MHD drive and normalized rotation
 - $q=2$ surface plays prominent role in stabilization mechanism
- **Quantitative agreement of RFA in DIII-D and JET**
 - Increase of RFA above $\beta_{\text{no wall}}$ in qualitative agreement with NSTX
 - RFA is manifestation of a weakly damped RWM
- **Aspect ratio dependence of $\Omega_{\text{crit}}\tau_A$ in DIII-D and NSTX explained by trapped particles not contributing to RWM stabilization**
 - Alternatively, the stabilization is determined by the sound wave velocity rather than the Alfvén wave velocity

